Improved Conductivity of Carbon Nanotube Networks by *In Situ* Polymerization of a Thin Skin of Conducting Polymer

Yufeng Ma,[†] William Cheung,[†] Dongguang Wei,[‡] Albert Bogozi,[§] Pui Lam Chiu,[†] Lin Wang,[†] Francesco Pontoriero,[†] Richard Mendelsohn,[†] and Huixin He[†,*]

[†]Chemistry Department, Rutgers University, Newark, New Jersey 07102, [‡]Carl Zeiss SMT, Inc. One Corporation Way, Peabody, Massachusetts 01960, and [§]Air Force Research Laboratories, Wright-Patterson Air Force Base, Ohio 45433

ABSTRACT The overall conductivity of SWNT networks is dominated by the existence of high resistance and tunneling/Schottky barriers at the intertube junctions in the network. Here we report that *in situ* polymerization of a highly conductive self-doped conducting polymer "skin" around and along single stranded DNA dispersed and functionalized single wall carbon nanotubes can greatly decrease the contact resistance. The polymer skin also acts as "conductive glue" effectively assembling the SWNTs into a conductive network, which decreases the amount of SWNTs needed to reach the high conductive regime of the network. The conductance of the composite network after the percolation threshold can be 2 orders of magnitude higher than the network formed from SWNTs alone.

KEYWORDS: conducting polymer · polyaniline · carbon nanotubes · nanocomposite

There is increasing enthusiasm for the use of single-walled carbon nanotube (SWNT) networks as conductive flexible electrodes and sensing materials because of the following advantages: SWNT films can be readily fabricated by several room temperature solution-based processes, such as spray coating,[1,2] inkjet printing,[3,4] deposition through a filter, [5,6] and deposition by a layer-by-layer approach.[7,8] The obtained network electrodes are highly reproducible owing to statistical averaging effects and exhibit percolation-like electrical conductivity. SWNT networks have been demonstrated to function for a variety of applications including electrodes for solar cells,[9] organic light emitting diode,[10] smart windows,[11] sensors,[12] and transparent transistors.[2] There have been several reports on the conductivity of SWNT networks with values ranging from 12.5 S/cm[13] to ~6600 S/cm.[5,14] The discrepancy in these values are due to many factors that can affect the conductivity of SWNT networks, including inhomogeneous distribution of SWNTs with respect to length, diameter, the doping level of the tubes,[6,15–17] and the metallic-to-semiconducting SWNT volume fraction. Nevertheless, all the experimentally measured conductivities of the SWNT networks are significantly lower than the conductivity of a SWNT rope (axial conductivity ~10000 to 90000 S/cm).[18,19] Previous measurements also show that the conductivity of SWNT networks decreases as the temperature drops.[14] The low conductivity and the strong temperature dependence indicate the existence of high resistance and tunneling/Schottky barriers at the intertube junctions, which dominate the overall film conductivity in the network. One could expect that decreasing the intertube resistance could increase the conductivity of the network. Indeed, Lee and co-workers[20] reported that contact junctions can be improved by removing the insulating surfactant in SWNT networks with a 12 M HNO_3 treatment. Consequently, the conductivity of the SWNT network increased 2.5 times.

Inspired by the remarkable electronic and thermal conductivity and the superior mechanical properties of carbon nanotubes (CNTs), tremendous efforts have been made over the past decade to prepare polymer and CNT composites with an aim of synergistically combining the merits of each individual component.[8,21–28] However, although most of the reported composites show enhancement over polymeric materials, much lower electronic performance is observed when compared to CNT films.[14] Recently, Sun *et al.*[29] demonstrated that bulk-separated metallic SWNTs offered

*Address correspondence to huixinhe@newark.rutgers.edu.

Received for review March 30, 2008 and accepted May 20, 2008.

Published online June 6, 2008.
10.1021/nn800201n CCC: $40.75

superior performance than the as-produced nanotube sample in conductive composites prepared by blending with poly(3-hexylthiophene) and also poly(3,4-ethylene dioxythiophene):poly(styrene sulfonate). The author did not compare the performance of films prepared from SWNTs alone. Blanchet *et al.*[30] discovered that the percolation threshold of a SWNT network was dramatically downshifted upon replacing the insulating dispersing reagents in the network with a conducting polymer. However, after percolation, the conductivity of the SWNT network was not increased by the replacement.

Herein, we report that the conductivity of SWNT networks can be dramatically improved by *in situ* polymerization of a thin layer of self-doped conducting polymer (polyaniline boronic acid, PABA) around and along the carbon nanotubes. The formed conducting polymer improves the contacts between the SWNTs and it also acts as a conductive "glue" or "zipper", which effectively assembles the SWNTs into a conductive network and decreases the amount of SWNTs needed to reach the high conductive regime of the network. The conductance of the composite network beyond the percolation threshold can be 2 orders of magnitude higher than the network formed from SWNTs alone. In addition, the thin layer of conducting polymer provides a powerful functionality for a variety of potential applications,[11,31] including flexible sensors.[28,32–36]

However, we found that only *in situ* polymerized conducting polymers were able to effectively interlink the SWNTs to form a highly conductive network. The preformed conducting polymer dramatically decreased the conductivity and increased the percolation threshold of the SWNT networks. Surprisingly, the conducting polymer formed by *in situ* polymerization with preoxidized SWNTs ("seed" method) did not assemble the nanotubes into a conductive network either. Instead, the polymer induced severe aggregation of the nanotubes into large particles. Consequently, the percolation threshold of the composite formed by the seed approach is much higher and the conductance after the percolation threshold is 3 orders of magnitude lower than the network formed by SWNTs alone.

RESULTS AND DISCUSSION

Electrical Properties of the Composite and ss-DNA/SWNT Films. The conductance of networks formed from randomly arranged conducting sticks (CSs) exhibits a percolation behavior.[37] The electrical conductivity of the network increases sharply by orders of magnitude when the concentration of the CSs in the network reaches its percolation threshold. Above the percolation threshold, electrons conduct predominantly along the CS and move directly from one CS to the next.

Because of their high electrical conductivities and large aspect ratios, the electrical conductivities of carbon nanotubes films[14,38] and carbon nanotube/polymer composites[29,30,39] have been understood according to the percolation theory of randomly arranged CSs. Figure 1a shows the room-temperature percolation behavior of the ss-DNA/SWNTs network and the composite films fabricated by different approaches described in the experimental section (*in situ* polymerized, "seed", and postmixture composites). The SWNT concentration of these solutions was kept constant at 10 mg/L.

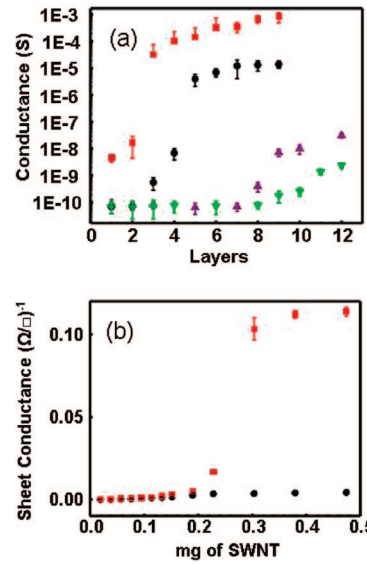

Figure 1. (a) Conductance of *in situ* polymerized composite (red square), ss-DNA/SWNTs (black dot), post mixture (purple triange), and "seed" composite (green inverted triangle) as a function of layers of the composites and ss-DNA/SWNTs. Each layer corresponds to 2 μL of solution with a concentration of SWNT at 10 mg/L. The conductance was measured by a two-probe approach. Each data point presented here was an average of 18 pair of electrodes on five silicon chips. (b) Conductance of *in situ* polymerized composite (red square), ss-DNA/SWNTs (black dot) measured by a four probe approach. These films of ss-DNA/SWNTs and composites with different thickness were fabricated through a vacuum filtration method. The conductance of "seed" composite and postmixture was beyond the sensitivity of the measurement setup. Each data point presented here was an average of 10 measurements.

At the third layer, the *in situ* fabricated composite reaches its percolation threshold while the ss-DNA/SWNT film just begins to have measurable current. At this percolation point, the conductance of the *in situ* polymerized composite is 5 orders of magnitude higher than that of the ss-DNA/SWNT film. There is no detectable current for the composites prepared by postmixing and "seed" method. According to the percolation mechanism, multiple conducting channels have formed in the *in situ* polymerized composite film and the tube-tube junctions begin to dominate its overall resistance, whereas space between conducting sticks is still the governing factor for the other three samples.

The films reached their percolation threshold at 3, 6, 10, and 11 layers for *in situ* polymerized composite, ss-DNA/SWNTs, postmixture, and seed composite, respectively. After percolation, the conductance of the *in situ* polymerized composite is $\sim 10^2$-fold, $\sim 10^5$-fold,

and ~10^6-fold higher than that of the ss-DNA/SWNTs, postmixture, and seed composite, respectively. Based on the percolation theory for randomly arranged conducting sticks, above the percolation threshold, the overall resistance of the film is dominated by intertube junctions in the conducting channels. The significant difference in conductance illustrates that only the *in situ* polymerized PABA remarkably improved the intertube contacts, while the preformed PABA and the *in situ* polymerized PABA by seed approach did not.

To eliminate the influence of electronic contacts between the electrodes and the composite on the electrical measurements, the percolation behavior of the *in situ* polymerized composite and ss-DNA/SWNTs alone were also studied by a four-probe approach. The distance between each probe is 1 mm. The conductance of the composite prepared by the seed method and postmixture approach is beyond the sensitivity of the measurement setup. Figure 1b shows that the sheet conductance of the *in situ* polymerized composite network increased 40 times compared to that of ss-DNA/SWNT alone. This number is lower than that measured by the two-probe setup on silicon chips. In contrast to two-probe measurements, it seems that the *in situ* polymerized conducting polymer skin did not decrease the amount of SWNTs needed to reach the high conductive regime of the network. This discrepancy may be related to the geometry-dependent percolation behavior of the carbon nanotube networks, which has been studied by Kumar *et al*. and Ural *et al*. recently.[40,41] With larger distances between the source and drain electrodes, the percolation probability of the carbon nanotubes, defined as the probability of finding at least one conducting path between the source and drain electrodes, decreased more dramatically compared to the small ones. In this work, the distance between the two electrodes is around 2 μm in the two-probe measurement, 500 times shorter than the distance between the probes in the four-probe measurements (1 mm). It is possible that the length of the "glued" tubes by self-assembling during the polymerization is still too short compared to 1 mm, while it is comparable or longer than 2 μm. Atomic force microscopic study of the films supports this hypothesis, which will be discussed in the morphology study section of this work. Therefore, the "glue" effect dramatically facilitates the percolation in the two-probe measurement, while not too effective for the four-probe measurements. The detailed geometry-dependent percolation behavior of the composite network is still under investigation in our group, nevertheless, this study demonstrates that *in situ* polymerization of a thin layer of conducting polymer could effectively improve the contact between the tubes and increase the overall conductivity of the carbon nanotube network. On the contrary, the postmixture and seed approach did not improve, but in fact, dramatically decreased the conductance of the ss-DNA/SWNT network.

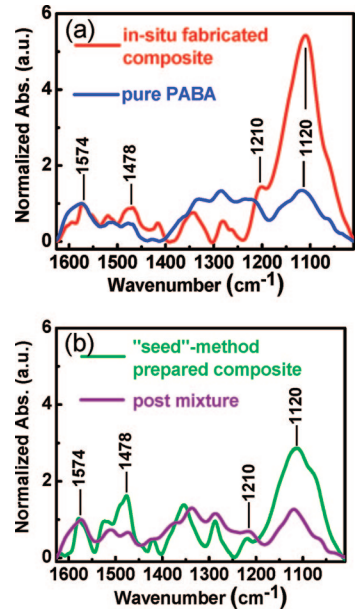

Figure 2. Normalized Fourier-transform IR spectra of (a) *in situ* polymerized composite (red) and pure PABA (blue); (b) seed composite (green) and postmixture (purple). After the baseline correction at two points (1626 and 1010 cm^{-1}), all IR spectra are normalized as the standard peak (quinoind) at 1574 cm^{-1}.

Molecular Structures of PABA in the Composites. Recently, we found that the polymerization kinetics and the electronic structure of poly(aniline boronic acid) (PABA) in the composite prepared by *in situ* polymerization are very different from that of neat PABA and the PABA in the composite prepared by seed approach.[42] Our first assumption is that the molecular and electronic structures of PABA in the composites fabricated by various approaches are different, which might be the reason for the observed dramatically different conductance and percolation behaviors. We used Fourier transform infrared (FTIR) spectroscopy to systematically study the molecular structures of PABA in the composites.

Figure 2 shows the FTIR spectra of the four samples: *in situ* polymerized composite, neat PABA, seed-composite, and postmixture. IR characteristic bands of polyaniline are observed at 1574, 1478, and 1120 cm^{-1}, corresponding to quinoid, benzenoid, and C=N stretching (−N═quinoid═N−, "electron-like band"[43]) modes, respectively.[23,43,44] The peak at 1210 cm^{-1} is related to the antisymmetric stretching vibration of the PO^{2-} in DNA.[45] The spectra also exhibit characteristic vibrations at 1510 and 1340 cm^{-1}, assigned to the B−N and B−O stretching mode.[46] The calculated ratio for the absorption intensity of quinoid to benzenoid ring modes (I_{1574}/I_{1478}) in the pure PABA is 3.5 (Table 1), which suggests that the percentage of quinoid units is much higher than that of benzenoid units for the neat PABA film. However, the ratio of I_{1574} to I_{1478} decreases to 1.5 for PABA in the *in situ* fabricated composite, indicating

TABLE 1. Intensity Ratio of Quinoind and Benzenoid Units and Relative Intensity of "Electron-like Band" (−N═quinoid═N−) for Pure PABA and Three Different Composites[a]

samples	intensity ratio I_{1574}/I_{1478}	relative intensity of −N═quinoid═N− stretching at 1120 cm^{-1}
pure PABA	3.5	1.3
in situ fabricated composite	1.5	5.4
post mixture	3.4	1.3
seed-method prepared composite	0.9	2.9

[a]The peak intensity reading is similar to that in ref 39.

that the relative amount of quinoid units decreased in the PABA when polymerized in the presence of ss-DNA/SWNTs. This result is consistent with our previous work,[47] indicating that the PABA exists more in the fully oxidized pernigraniline state in the pure PABA and more in the conductive emeraldine state in the composite. We hypothesized that this phenomenon is related to the electron-donating ability of the DNA molecules.[48] Because of the ss-DNA functionalization, the SWNTs become effective electron donors and therefore possess reductive capability.[49] Pernigraniline produced during the polymerization was readily reduced to the emeraldine state by the ss-DNA/SWNTs (Scheme 1).

The ratio of relative intensities of quinoid to benzenoid ring modes (I_{1574}/I_{1478}) in the post mixture is 3.4, which is similar to the neat PABA (3.5), indicating that the neat PABA weakly interacts with the ss-DNA/SWNTs in the composite. The results demonstrate that the PABA in the postmixture composite exists in the nonconductive pernigraniline state.

A striking difference among the four spectra in Figure 2 is found in −N═quinoid═N− stretching at ~1120 cm^{-1}. The peak has been described by MacDiarmid *et al.*[43,50] as the "electronic-like band" and is considered to be a measure of the degree of delocalization of electrons along the polyaniline backbone, and thus it is a characteristic peak of polyaniline conductivity. There is a dramatic increase intensity of the

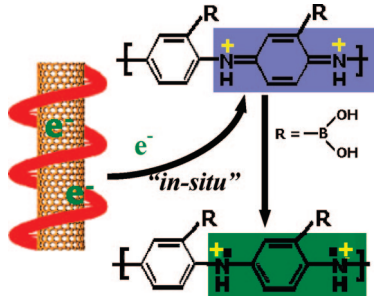

Scheme 1. ss-DNA Functionalized Single-Walled Carbon Nanotube (SWNT). The schematic is only a graphical presentation and does not represent the precise way that ss-DNA binds on SWNTs. Because of the electron richness of the ss-DNA/SWNTs, the pernigraniline state of PABA produced during the polymerization is readily reduced to the stable and conductive emeraldine state.

"electronic-like band" in the *in situ* polymerized composite, as shown in Figure 2a and Table 1. This remarkable increase suggests that PABA in the *in situ* polymerized composite has higher conductivity compared to the neat PABA. The composite fabricated by the post-mixture approach shows similar low intensity of the "electron-like band" as the neat PABA, indicating that conductivity of the PABA in the postmixture composite may be similar to the neat PABA.

Unexpectedly, the relative intensity of the "electron-like band" in the composite prepared by the seed approach is 2.9, much higher than that of the neat PABA and the postmixture composite (1.3). The ratio of relative intensities of quinoid to benzenoid ring modes (I_{1574}/I_{1478}) in the composite prepared seed-method is 0.9, much lower than that of the neat PABA and the postmixture composite (3.5 and 3.4, respectively). The results indicated that the PABA in the composite fabricated by the seed approach also existed in the conductive emeraldine states. Therefore, the conductivity of the PABA should be higher than the PABA in the postmixture composite, even though lower than that of the composite prepared by *in situ* polymerization with the intact ss-DNA/SWNTs. However, the conductance measurements described above did not show this trend, indicating that there are other uncovered factors that determine the overall macroscopic conductivity of the films in addition to the modified tube−tube contacts. To understand the percolation behaviors of the composites, we further studied the morphology of the films and the spatial distribution of the carbon nanotubes in the films at different percolation states.

Morphology Studies. Atomic force microscope (AFM) and high resolution transmission electron microscope (HRTEM) images in Figure 3 show the third layer of the different samples (ss-DNA/SWNTs, *in situ* polymerized composite, postmixture and seed composite) that have been prepared layer-by-layer from the corresponding solutions with a SWNT concentration of 10 mg/L. At this percolation point, as shown in Figure 1a, only the composite fabricated by *in situ* polymerization with the intact ss-DNA/SWNTs reached the percolation threshold studied by two-probe measurements. The composites fabricated by postmixture and seed method showed no detectable current by our detection instruments. Figure 3a shows the morphology of the films prepared from ss-DNA/SWNT alone. Most of the SWNTs are individual (~2 nm in diameter), with some bundled structures (~17 nm). The nanotubes appear randomly oriented. Most of the tubes remain isolated from each other, with some jointed tubes.

Figure 3b is a typical AFM image of the *in situ* polymerized composite. Remarkably, individual ss-DNA/SWNTs are replaced by long fibers (most of the fibers are longer than 4 μm). These fibers are randomly arranged and self-assembled into a network. The diameter of the fibers ranges from 3 to 20 nm measured by

high resolution TEM (Figure 3c). From the TEM images it is noted that some of the fibers are composed of individual nanotubes with a polymer coating of 1 to 3 nm in thickness. Some of the fibers are carbon nanotube bundles, which are composed of carbon nanotubes with polymer coating. The prepolymerized PABA did not show the tendency to self-assemble the carbon nanotubes into networks (Figure 3d). The arrangement and the spatial distribution of the carbon nanotubes in the postmixture composite are very similar to that of ss-DNA/SWNT alone. In the AFM image, there are large bright regions (~60 nm in height), which are suspected to be the neat PABA without being uniformly mixed with the SWNTs. From the study by high resolution TEM (Figure 3g), we found that while some of the tubes were not coated, some were coated with a 1−3 nm layer of polymer.

In the conductance experiment, we found the conductance of the postmixture network dramatically decreased and the percolation threshold of the SWNT networks largely increased (3 fold) (Figure 1). After the percolation threshold, the conductance of the postmixture composite is 3 orders of magnitude lower than the network prepared from SWNT alone, and is 5 orders of magnitude lower than the network formed from the *in situ* polymerized PABA composite. Combined with the FTIR results, showing that the PABA exists in the nonconductive pernigraniline state in the postmixture composite and in the conductive emeraldine state in the *in situ* polymerized composite, this morphological study strongly suggests that the electronic and molecular structure and therefore the conductivity of the interfacial PABA on the SWNTs can modulate the overall electronic performance and percolation behavior of the SWNT films. Compared to the simple postmixture process, the *in situ* polymerization process also facilitates SWNTs self-assembling to highly conducting networks, which also largely contributes to the highly improved conductance and the low percolation threshold of the *in situ* polymerized composite. This result soundly supports the hypothesis discussed earlier in this work.

The morphological study of the seed composite (Figure 3e,f) revealed our curiosity pertaining to why the conductance is even lower than the postmixture. In contrast to the PABA *in situ* polymerized in the presence of the intact ss-DNA/SWNTs, the PABA in the seed composite did not interlink the nanotubes into a conductive network. Instead, the PABA induced severe aggregation of the nanotubes into large particles (as large as 1 μm). The aggregation mechanism is still under investigation. It is possibly related to defects along the tubes caused by the preoxidation process, which largely weakens the mechanical strength of the carbon nanotube. We suggest that the PABA was first formed on the carbon nanotubes, indicated by the polymer agglomerates (~35 nm in height) attaching on each isolated nanotube (Figure 3e). These agglomerates further induce the carbon nanotubes to curl into larger particles[51] (Figure 3f). This aggregation dramatically changed the effective length/diameter aspect ratio of the carbon nanotubes, which is known to impact the conductivity and percolation behavior of the carbon nanotube films.[52] Therefore, even though the PABA in the seed composite may have higher conductivity compared to that of PABA in the postmixture, the aggregated carbon nanotubes make the conductivity of the seed composite even lower than the postmixture composite. Therefore, we conclude that not only the molecular structure of the polymer but also the arrangement or distribution of carbon nanotubes in the composites determines the overall macroscopic electronic property and percolation behavior of the composites.

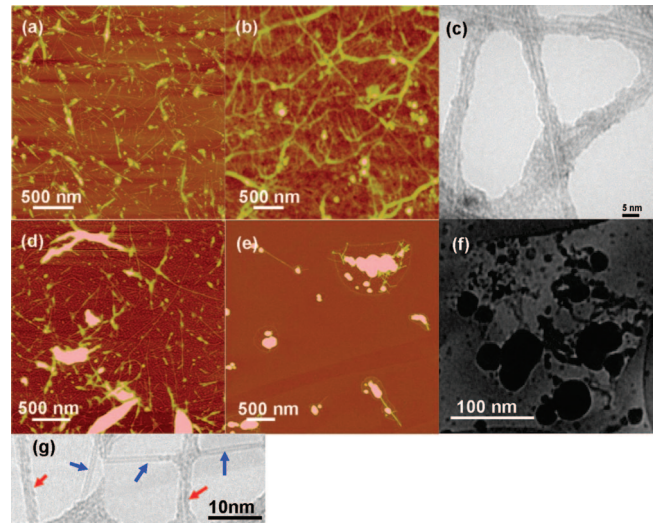

Figure 3. AFM images of the third layers of the films prepared from (a) ss-DNA/SWNTs, (b) *in situ* polymerized composite, (d) postmixture, and (e) seed composite. The concentration of SWNT in all these samples is 10 mg/L. TEM images of *in situ* polymerized composite (c), seed composite, (f) and postmixture (g).

SUMMARY

The electrical performance of SWNT network can be significantly improved by *in situ* polymerization of a thin layer of PABA on the intact ss-DNA/SWNTs. The thin layer of PABA also acts as a conductive "glue" or "zipper", which can effectively assemble the ss-DNA/SWNTs into a conductive network. These advantages cannot be obtained by simply mixing a preformed conducting polymer with the ss-DNA/SWNTs. Surprisingly, we also found that the enhancement was not achievable by *in situ* polymerization with preoxidized SWNTs (seed method). The fabrication process rigorously impacts the electronic and molecular structure of the produced PABA in the composites, and also the arrangement or lateral distribution of the carbon nanotubes in the composites. Understanding these reaction characteristics is important to effectively optimize the fabrication parameters and ensure the formation of SWNT networks in a controllable fashion for a variety of potential applications.

METHODS AND MATERIALS

Materials. 3-Aminophenylbronic acid hemisulfate salt (ABA), potassium fluoride (KF) and all other chemicals were purchased from Aldrich and used as received. Single-stranded DNA (ss-DNA) with sequence $d(T)_{30}$ was purchased from Integrated DNA Technologies. All solutions were prepared using deionized water (18.2 MΩ) (Nanopore water, Barnstead).

Dispersion and Functionalization of SWNTs with Single-Stranded DNA. HiPco Purified single-walled carbon nanotubes (SWNTs) were purchased from Carbon Nanotechnologies and dispersed into water using the method described by Zheng *et al.*[53] It was reported that the ss-DNA binds to the carbon nanotubes through π stacking, resulting in helical wrapping to the surface of the carbon nanotubes.[53] Briefly, 11 mg of purified HiPco SWNT was suspended in aqueous ssDNA solution. This mixture was kept at 0 °C with an ice−water bath and sonicated with a Sonics Vibra-cell (at 30% amplitude) for 30 min. After sonication, the sample was centrifuged with a Beckman centrifuge at 5000 g to remove undispersed SWNTs. As a result, highly dispersed and ss-DNA functionalized SWNT (ss-DNA/SWNT) solution was obtained. To remove free ss-DNA in the dispersed solution, the solution was dialyzed with a microcon YM-100 centrifugal filter unit (Millipore) for 4 h. The electronic structure of the ss-DNA/SWNTs was studied with a Cary 500 UV−vis−NIR spectrophotometer using double beam mode.

Different Approaches to Fabricate ss-DNA/SWNT/Polyaniline Boronic Acid (ss-DNA/SWNT/PABA) Composite Solutions. Recently, we fabricated a highly conductive self-doped polyaniline/SWNT composite by *in situ* polymerization (both chemical and electrochemical polymerization) of 3-aminophenylboronic acid (ABA) monomers in the presence of the ss-DNA/SWNTs.[34,47] We found that the ABA polymerization speed was dramatically increased (4500 times) by adding 1% (by weight) of ss-DNA/SWNTs into the polymerization solution. The formed polyaniline boronic acid (PABA) preferentially deposited on the carbon nanotubes.[42] More importantly, the quality of the PABA was significantly improved, as indicated by the fact that the PABA backbone had longer conjugation length and existed in the more stable and conductive emeraldine state.[42,47]

Adding ss-DNA alone into the solution only slightly increased the polymerization speed (3 times), and the conjugation length of the formed PABA was similar to the neat PABA formed in the absence of ss-DNA or ss-DNA/SWNTs, indicated by the UV−vis−NIR electronic absorption spectra. Furthermore, our previous atomic force microscopy (AFM) study demonstrated that double stranded-DNA (ds-DNA) molecules could be used as templates to fabricate polyaniline nanowires on insulating substrates,[54] a procedure that relies on the electrostatic attraction of protonated aniline monomers to the negative charges along a DNA template. However, ds-DNA alone was not able to act as a molecular template to form PABA nanowires, possibly due to the steric effect of the boronic acid groups in the ABA monomers.[34] In contrast, nanowires of PABA can be fabricated by using ss-DNA/SWNTs as growing templates. Since the electrostatic attraction provided by the phosphate groups was not strong enough to emulsify and align the monomers of 3-aminophenylboronic acid, we believe that the strong π−π interaction between the monomeric benzene ring and the graphite regions on the carbon nanotube played an especially important role in preconcentrating the 3-aminophenylboronic acid monomers before the polymerization.

The mechanism for the polymerization of aniline and aniline derivatives has been proposed as oxidative polymerization.[55] We hypothesize that the ABA monomers were preconcentrated along the ss-DNA/SWNTs and formed SWNT · ABA complexes, which act as polymerization precursors. Due to the electron donating ability of the DNA molecules, the ss-DNA/SWNTs become highly electron rich,[49] which increases the electron density of the ABA monomers, and facilitates the polymerization. By adding the oxidant, $(NH_4)_2S_2O_8$ (APS), into the ss-DNA/SWNTs solution before introduction of the ABA monomers, the ss-DNA/SWNTs was oxidized and became electron deficient. We indeed found that the polymerization of ABA was dramatically slowed down even though it has been reported that oxidized SWNTs could lead to the production of conducting polymer nanowires, which is known as "seed" method.[56,57] Furthermore, the electronic and molecular structure of the produced PABA in the composite was very different from the PABA in the composites fabricated with the intact ss-DNA/SWNTs.[42]

On the basis of these previous studies, we fabricated ss-DNA/SWNT/PABA composite solutions using different fabrication approaches to study how the fabrication process impacts the electronic performance of the composite networks. A typical procedure for the preparation of a solution of ss-DNA/SWNT/PABA nanocomposite by an *in situ* polymerization approach is as follows: 50 μL of ABA solution (50 mM) and KF (40 mM) in 0.05 M H_2SO_4 was added to 2.5 mL of the ss-DNA/SWNTs solution (70 mg/L) in 0.05 M H_2SO_4. The solution was bubbled with nitrogen for 30 min at 0 °C to remove the dissolved oxygen. The chemical polymerization of ABA was then initiated by adding 11.34 μL of 37.5 mM $(NH_4)_2S_2O_8$ (APS) (in 0.05 M H_2SO_4) dropwise to the mixture. It is important to note that the amounts of ABA and APS were determined from titration experiments to make sure only a thin layer of PABA is produced around and along the carbon nanotubes (Figure S1, Supporting Information). The polymerization was carried out at 0 °C with nitrogen bubbling for 7 h and another 43 h in a refrigerator (4 °C). The obtained composite solution is referred to as "*in-situ* polymerized composite". For the "seed" approach,[56,57] the polymerization conditions were kept the same, except 11.34 μL of 37.5 mM APS was first added to preoxidize the same amount of ss-DNA/SWNTs, followed by addition of 50 μL of ABA solution (50 mM). The obtained composite solution is termed "seed composite". A neat poly(aniline boronic acid) (PABA) was fabricated by a recipe described in our previous work, which was demonstrated to produce PABA with longer conjugation length.[47] A composite of ss-DNA/SWNT/PABA was prepared by mixing 50 μL of the preformed neat polymer solution with 2.5 mL of the ss-DNA/SWNTs (70 mg/L) in 0.05 M H_2SO_4. The resulting solution is so-called "postmixture composite". All the composites, neat PABA, and ss-DNA/SWNTs solutions were dialyzed to remove excess salts before conductance measurements.

Conductance Measurements. Percolation-like conductive behaviors of the composites prepared as described above and ss-DNA/SWNT alone were studied by measuring the conductance of the films in a layer-by-layer approach on a prepatterned Si chip. Each layer was prepared by adding 2 μL of the dialyzed solution (10 mg/L of SWNTs) onto a Si chip and dried under vacuum. The Si chip was fabricated at Air Force Research Laboratories, and the distance between two facing gold electrodes is 2 μm. Then, the conductance of the composites was measured with an Electrochemical Workstation CHI 760C.

To eliminate the influences of contact resistance between the composite and the electrodes during measurements, the percolation-like conductive behaviors of the composites and ss-DNA/SWNTs alone were also studied by a four-probe approach. Films with different thickness were prepared from the corresponding composite and ss-DNA/SWNT solutions by vacuum filtration using Anodisc 47 inorganic membranes with 200 nm pores (Whatman Ltd.). To evaluate the impact of the conducting polymer skin on the conductivity of the carbon nanotube network, the thickness of each film was prepared with different composite solutions while maintaining the concentration of the carbon nanotubes (note that the film thickness for different composites will be slightly different). After filtration, the thin films were dried in vacuum for 15−20 min. The sheet conductance of the films was determined by a 302 manual four point resistivity probe (Lucas Laboratories).

Characterization. The morphology of the resulting composites, neat polymer, and the ss-DNA/SWNT films was characterized by a Nanoscope III A (Digital Instruments) operating with tapping mode in ambient air. The thickness of PABA on the carbon nanotubes was measured from high-resolution transmission electron microscope (TEM) (Libra 120 Energy Filtering TEM, Zeiss) operated at 200 kV. Samples were prepared for imaging by placing a drop of aqueous composite solution on TEM grids and wicking away the liquid after 2 min. The molecular structures of the PABA in the pure polymer and the composites were measured

by Fourier transform infrared (FTIR) spectroscopies. The FTIR spectra were recorded on a Spectrum Spotlight FTIR imaging system (Perkin-Elmer instruments).

Acknowledgment. This material is based upon work supported by the National Science Foundation under Grant CHE-0750201 and Petroleum Research Fund.

Supporting Information Available: Titration by UV−vis spectroscopy to optimize the ABA concentration for coating a thin layer of PABA around and along the ssDNA/SWNTs. This material is available free of charge *via* the Internet at http://pubs.acs.org.

REFERENCES AND NOTES

1. Kaempgena, M.; Duesbergb, G. S.; Rotha, S. Transparent Carbon Nanotube Coatings. *Appl. Surf. Sci.* **2005**, *252*, 425–429.
2. Artukovic, E.; Kaempgen, M.; Hecht, D. S.; Roth, S.; Gruner, G. Transparent and Flexible Carbon Nanotube Transistors. *Nano Lett.* **2005**, *5*, 757–760.
3. Kordás, K.; Mustonen, T.; Tóth, G.; Jantunen, H.; Soldano, C.; Talapatra, S.; Kar, S.; Vajtai, R.; Ayayan, P. Inkjet Printing of Electrically Conductive Patterns of Carbon Nanotubes. *Small* **2006**, *2*, 1021–1025.
4. Simmons, T. J.; Hashim, D.; Vajtai, R.; Ajayan, P. M. Large Area-Aligned Arrays From Direct Deposition of Single-Wall Carbon Nanotube Inks. *J. Am. Chem. Soc.* **2007**, *129*, 10088–10089.
5. Wu, Z.; Chen, Z.; Du, X.; Logan, J. M.; Sippel, J.; Nikolou, M.; Kamaras, K.; Reynolds, J. R.; Tanner, D. B.; Hebard, A. F. Transparent, Conductive Carbon Nanotube Films. *Science* **2004**, *305*, 1273–1276.
6. Zhang, D.; Ryu, K.; Liu, X.; Polikarpov, E.; Ly, J.; Tompson, M. E.; Zhou, C. Transparent, Conductive, and Flexible Carbon Nanotube Films and Their Application in Organic Light-Emitting Diodes. *Nano Lett.* **2006**, *6*, 1880–1886.
7. Shim, B. S.; Tang, Z.; Morabito, M. P.; Agarwal, A.; Hong, H.; Kotov, N. A. Integration of Conductivity, Transparency, and Mechanical Strength into Highly Homogeneous Layer-by-Layer Composites of Single-Walled Carbon Nanotubes for Optoelectronics. *Chem. Mater.* **2007**, *19*, 5467–5474.
8. Kovtyukhova, N. I.; Mallouk, T. E. Ultrathin Anisotropic Films Assembled from Individual Single-Walled Carbon Nanotubes and Amine Polymers. *J. Phys. Chem. B* **2005**, *109*, 2540–2545.
9. Rowell, R. W.; Topinka, M. A.; McGehee, M. D.; Prall, H.-J.; Dennler, G.; Sariciftci, N. S.; Hu, L.; Gruner, G. Organic Solar Cells with Carbon Nanotube Network Electrodes. *Appl. Phys. Lett.* **2006**, *88*, 233506.
10. Li, J.; Hu, L.; Wang, L.; Zhou, Y.; Gruner, G.; Marks, T. J. Organic Light-Emitting Diodes Having Carbon Nanotube Anodes. *Nano Lett.* **2006**, *6*, 2472–2477.
11. Gruner, G. Carbon Nanotube Films for Transparent and Plastic Electronics. *J. Mater. Chem.* **2006**, *16*, 3533–3539.
12. Ferrer-Anglada, N.; Kaempgen, M. S. R. Transparent and Flexible Carbon Nanotube/Polypyrrole and Carbon Nanotube/Polyaniline pH Sensors. *Phys. Status Solidi B* **2006**, *243*, 3519–3523.
13. Meitl, M. A.; Zhou, Y.; Gaur, A.; Jeon, S.; Usrey, M. L.; Strano, M. S.; Rogers, J. A. Solution Casting and Transfer Printing Single-Walled Carbon Naontube Films. *Nano Lett.* **2004**, *4*, 1643–1647.
14. Bekyarova, E.; Itkis, M. E.; Cabrera, N.; Zhao, B.; Yu, A. P.; Gao, J.; Haddon, R. C. Electronic Properties of Single-Walled Carbon Nanotube Networks. *J. Am. Chem. Soc.* **2005**, *127*, 5990–5995.
15. Dettlaff-Weglikowska, U.; Skákalová, V.; Graupner, R.; Jhang, S. H.; Kim, B. H.; Lee, H. J.; Ley, L.; Park, Y. W.; Berber, S.; Tománek, D. Effect of $SOCl_2$ Treatment on Electrical and Mechanical Properties of Single-Wall Carbon Nanotube Networks. *J. Am. Chem. Soc.* **2005**, *127*, 5125–5131.
16. Parekh, B. B.; Fanchini, G.; Eda, G.; Chhowalla, M. Improved Conductivity of Transparent Single-Wall Carbon Nanotube Thin Films *via* Stable Postdeposition Functionalization. *Appl. Phys. Lett.* **2007**, *90*, 121913.
17. Fanchini, G.; Unalan, H. E.; Chhowalla, M. Modification of Transparent and Conducting Single Wall Carbon Nanotube Thin Films *via* Bromine Functionalization. *Appl. Phys. Lett.* **2007**, *90*, 092114.
18. Thess, A.; Lee, R.; Nikolaev, P.; Dai, H. J.; Petit, P.; Robert, J.; Xu, C. H.; Lee, Y. H.; Kim, S. G.; Rinzler, A. G. Crystalline Ropes of Metallic Carbon Nanotubes. *Science* **1996**, *273*, 483–487.
19. Mann, D.; Javey, A.; Kong, J.; Wang, Q.; Dai, H. J. Ballistic Transport in Metallic Nanotubes with Reliable Pd Ohmic Contacts. *Nano Lett.* **2003**, *3*, 1541–1544.
20. Geng, H.-Z.; Kim, K. K.; So, K. P.; Lee, Y. S.; Chang, Y.; Lee, Y. H. Effect of Acid Treatment on Carbon Nanotube-Based Flexible Transparent Conducting Films. *J. Am. Chem. Soc.* **2007**, *129*, 7758–7759.
21. Iijima, S. Helical Microtubules of Graphitic Carbon. *Nature* **1991**, *354*, 56–58.
22. Dai, L.; Mau, A. W. H. Controlled Synthesis and Modification of Carbon Nanotubes and C60: Carbon Nanostructures for Advanced Polymeric Composite Materials. *Adv. Mater.* **2001**, *13*, 899–913.
23. Zengin, H.; Zhou, W.; Jin, J.; Czerw, R.; Smith, J. D. W.; Echegoyen, L.; Carroll, D. L.; Foulger, S. H.; Ballato, J. Carbon Nanotube Doped Polyaniline. *Adv. Mater.* **2002**, *14*, 1480–1483.
24. Cochet, M.; Maser, W. K.; Benito, A. M.; Callejas, M. A.; Martínez, M. T.; Benoit, J.-M.; Schreiber, J.; Chauvet, O. Synthesis of a New Polyaniline/Nanotube Composite: "in-situ" Polymerisation and Charge Transfer through Site-Selective Interaction. *Chem. Commun.* **2001**, 1450–1451.
25. Li, X. H.; Wu, B.; Huang, J.-E.; Zhang, J.; Liu, Z. F.; Li, H. L. Fabrication and Characterization of Well-Dispersed Single-Walled Carbon Nanotube/Polyaniline Composites. *Carbon* **2002**, *411*, 1670–1673.
26. Bekyarova, E.; Davis, M. E.; Burch, T.; Itkis, M. E.; Zhao, B.; Sunshine, S.; Haddon, R. C. Chemically Functionalized Single-Walled Carbon Nanotubes as Ammonia Sensors. *J. Phys. Chem. B* **2004**, *108*, 19717–19720.
27. Ajayan, P. M.; Stephan, O.; Colliex, C.; Trauth, D. Aligned Carbon Nanotube Arrays Formed by Cutting a Polymer Eesin-Nanotube Composite. *Science* **1994**, *265*, 1212–1214.
28. Dai, L. M. Electrochemical Sensors Based on Architectural Diversity of the pi-conjugated Structure: Recent Advancements from Conducting Polymers and Carbon Nanotubes. *Aust. J. Chem.* **2007**, *60*, 472–483.
29. Wang, W.; Fernando, S.; Lin, Y.; Meziani, M. J.; Veca, L. M.; Cao, L.; Zhang, P.; Kimani, M. M.; Sun, Y.-P. Metallic Single-Walled Carbon Nanotubes for Conductive Nanocomposites. *J. Am. Chem. Soc.* **2008**, *130*, 1415–1419.
30. Blanchet, G. B.; Subramoney, S.; Bailey, R. K.; Jaycox, G. D.; Bnuckolls, C. Self-Assembled Three-Dimensional Conducting Network of Single-Wall Carbon Nanotubes. *Appl. Phys. Lett.* **2004**, *85*, 828–830.
31. Hall, D. G., Ed. *Boronic Acids: Preparation and Applications in Organic Synthesis and Medicine*; Wiley-VCH/Verlag GmbH & Co. KGaA: Weinheim, Germany, 2005.
32. Shoji, E.; Freund, M. S. Potentiometric Sensors Based on the Inductive Effect on the pKa of Polyaniline: A Nonenzymatic Glucose Sensor. *J. Am. Chem. Soc.* **2001**, *123*, 3383–3398.
33. Shoji, E.; Freund, M. S. Potentiometric Saccharide Detection Based on the pKa Change of Poly(aniline boronic acid). *J. Am. Chem. Soc.* **2002**, *124*, 12486–12493.
34. Ma, Y. F.; Ali, R. K.; Dodoo, A. S.; He, H. X. Enhanced Sensitivity for Biosensors: Multiple Functions of DNA Wrapped Single Walled Carbon Nanotubes in Self-Doped Polyaniline Nanocomposites. *J. Phys. Chem. B* **2006**, *110*, 16359–16365.
35. Ali, S. K.; Ma, Y. F.; Parajuli, R. R.; Balogan, Y.; Lai, W. Y.-C.; He, H. X. A Non-Oxidative Sensor Based on a Self-Doped Polyaniline/Carbon Nanotube Composite for Highly Sensitive and Selective Detection of the Neurotransmitter Dopamine. *Anal. Chem.* **2007**, *79*, 2583–2587.

36. Ali, S. K.; Parajuli, R. R.; Ma, Y. F.; Balogan, Y.; Lai, W. Y.-C.; He, H. X. The Interference of Ascorbic Acid in Dopamine Detection by a Non-Oxidative Approach. *J. Phys. Chem. B* **2007**, *111*, 12275–12281.
37. Pike, G. E.; Seager, C. H. Percolation and Conductivity: A Computer Study. I. *Phys. Rev. B* **1974**, *10*, 1421–1434.
38. Hu, L.; Hecht, D. S.; Grüner, G. Percolation in Transparent and Conducting Carbon Nanotube Networks. *Nano Lett.* **2004**, *4*, 2513–2517.
39. Winey, K. I.; Kashiwagi, T.; Mu, M. Improving Electrical Conductivity and Thermal Properties of Polymers by the Addition of Carbon Nanotubes as Fillers. *MRS Bull.* **2007**, *32*, 348−353.
40. Behnam, A.; Ural, A. Computational Study of Geometry-Dependent Resistivity Scaling in Single Walled Carbon Nanotube Films. *Phys. Rev. B* **2007**, *75*, 125432.
41. Kumar, S. K.; Murthy, J. Y.; Alam, M. A. Percolating Condition in Finite Nanotube Networks. *Phys. Rev. Lett.* **2005**, *95*, 066802.
42. Ma, Y. F.; Chiu, P. L.; Chen, A. M.; Serrano, A.; Ali, S. K.; He, H. X. The Electronic Role of DNA Functionalized Carbon Nanotubes: Efficacy for *in-Situ* Polymerization of Conducting Polymer Nanocomposite *J. Am. Chem. Soc.* **2008**, in press.
43. Quillard, S.; Louarn, G.; Lefrant, S.; MacDiarmid, A. G. Vibrational Analysis of Polyaniline: A Comparative Study of Leucoemeraldine, Emeraldine, and Pernigraniline Bases. *Phys. Rev. B* **1994**, *50*, 12496–12508.
44. Sainz, R.; Benito, A. M.; Martínez, M. T.; Galindo, J. F.; Sotres, J.; Baró, A. M.; Corraze, B.; Chauvet, O.; Maser, W. K. Soluble Self-Aligned Carbon Nanotube/Polyaniline Composites. *Adv. Mater.* **2005**, *17*, 278–281.
45. Nagarajan, R.; Liu, W.; Kumar, J.; Tripathy, S. K.; Bruno, F. F.; Samuelson, L. A. Manipulating DNA Conformation Using Intertwined Conducting Polymer Chains. *Macromolecules* **2001**, *34*, 3921–3927.
46. Recksiedler, C. L.; Deore, B. A.; Freund, M. S. A Novel Layer-by-Layer Approach for the Fabrication of Conducing Polymer/RNA Multilayer Films for Controlled Release. *Langmuir* **2006**, *22*, 2811–2815.
47. Ma, Y. F.; Ali, S. R.; Wang, L.; Chiu, P. L.; Mendelsohn, R.; He, H. X. *In-situ* Fabrication of A Water-Soluble, Self-Doped Polyaniline Nanocomposite: The Unique Role of DNA Functionalized Single-Walled Carbon Nanotubes. *J. Am. Chem. Soc.* **2006**, *128*, 12064–12065.
48. Kawamoto, H.; Uchida, T.; Kokima, K.; Tachibana, M. G Band Raman Features of DNA-Wrapped Single-Wall Carbon Nanotubes in Aqueous Solution and Air. *Chem. Phys. Lett.* **2006**, *432*, 172–176.
49. Zheng, M.; Diner, B. A. Solution Redox Chemistry of Carbon Nanotubes. *J. Am. Chem. Soc.* **2004**, *126*, 15490–15494.
50. Yan, X.-B.; Han, Z.-J.; Yang, Y.; Tay, B.-K. Fabrication of Carbon-Polyaniline Composites *via* Electrostatic Adsorption in Aqueous Colloids. *J. Phys. Chem. C* **2007**, *111*, 4125–4131.
51. Wang, Y. H.; Maspoch, D.; Zou, S. L.; Schatz, G. C.; Smalley, R. E.; Mirkin, C. A. Controlling the Shape, Orientation, and Linkage of Carbon Nanotube Features with Nano Affinity Templates. *Proc. Natl. Acad. Sci. U.S.A.* **2006**, *103*, 2026–2031.
52. Hecht, D.; Hu, L.; Grüner, G. Conductivity Scaling with Bundle Length and Diameter in Single Walled Carbon Nanotube Networks. *Appl. Phys. Lett.* **2006**, *89*, 133112.
53. Zheng, M.; Jagota, A.; Semke, E. D.; Diner, B. A.; Mclean, R. S.; Lustig, S. R.; Richardson, R. E.; Tassi, N. G. DNA-assisted Dispersion and Separation of Carbon Nanotubes. *Nat. Mater.* **2003**, *2*, 338–342.
54. Ma, Y. F.; Zhang, J. M.; Zhang, G. J.; He, H. X. Polyaniline Nanowires on Si Surfaces Fabricated with DNA Templates. *J. Am. Chem. Soc.* **2004**, *126*, 7097–7101.
55. Tzou, K.; Gregory, R. V. Kinetic Study of the Chemical Polymerization of Aniline in Aqueous Solutions. *Synth. Met.* **1992**, *47*, 267–277.
56. Zhang, X. Y.; Goux, W. J.; Manohar, S. K. Synthesis of Polyaniline Nanofibers by "Nanofiber Seeding". *J. Am. Chem. Soc.* **2004**, *126*, 4502–4503.
57. Zhang, X.; Manohar, S. K. Bulk Synthesis of Polypyrrole Nanofibers by a Seeding Approach. *J. Am. Chem. Soc.* **2004**, *126*, 12714–12715.